The EMBO Journal Vol. 20 No. 1 & 2 pp. 65–76, 2001

Role of elementary Ca^{2+} puffs in generating repetitive Ca^{2+} oscillations

Jonathan S.Marchant and Ian Parker[1]

Laboratory of Cellular and Molecular Neurobiology, Department of Neurobiology and Behavior, University of California Irvine, CA 92697, USA

[1]Corresponding author
e-mail: iparker@uci.edu

Inositol (1,4,5)-trisphosphate (IP_3) liberates intracellular Ca^{2+} both as localized 'puffs' and as repetitive waves that encode information in a frequency-dependent manner. Using video-rate confocal imaging, together with photorelease of IP_3 in *Xenopus* oocytes, we investigated the roles of puffs in determining the periodicity of global Ca^{2+} waves. Wave frequency is not delimited solely by cyclical recovery of the cell's ability to support wave propagation, but further involves sensitization of Ca^{2+}-induced Ca^{2+} release by progressive increases in puff frequency and amplitude at numerous sites during the interwave period, and accumulation of pacemaker Ca^{2+}, allowing a puff at a 'focal' site to trigger a subsequent wave. These specific 'focal' sites, distinguished by their higher sensitivity to IP_3 and close apposition to neighboring puff sites, preferentially entrain both the temporal frequency and spatial directionality of Ca^{2+} waves. Although summation of activity from many stochastic puff sites promotes the generation of regularly periodic global Ca^{2+} signals, the properties of individual Ca^{2+} puffs control the kinetics of Ca^{2+} spiking and the (higher) frequency of subcellular spikes in their local microdomain.

Keywords: Ca^{2+} oscillation/Ca^{2+} puffs/Ca^{2+} waves/ inositol trisphosphate/*Xenopus* oocyte

Introduction

In many different cell types, activation of the inositol (1,4,5)-trisphosphate (IP_3) second messenger pathway evokes repetitive spikes of cytosolic Ca^{2+}, arising as successive waves of Ca^{2+} that propagate throughout the cell (Fewtrell, 1993; Berridge and Dupont, 1994). These periodic Ca^{2+} signals encode information in a 'digital' manner, whereby the increasing strength of an extracellular stimulus results in an increasing frequency, but not amplitude, of intracellular Ca^{2+} spiking (Berridge and Dupont, 1994; Berridge, 1997a). For example, cellular responses as diverse as enzyme activation (De Koninck and Schulman, 1998), behavioral rhythms (Dal Santo *et al*., 1999) and gene transcription (Dolmetsch *et al*., 1997; Li *et al*., 1998) are regulated by Ca^{2+} spiking frequency. It is important, therefore, to elucidate the cellular mechanisms that generate periodic Ca^{2+} waves, and which thereby determine the relationship between [IP_3] and the frequency of Ca^{2+} oscillations.

A key feature is the well-established biphasic action of cytosolic Ca^{2+} in both facilitating and inhibiting the opening of IP_3 receptors (IP_3Rs), through which Ca^{2+} is liberated from the endoplasmic reticulum (ER) into the cytosol (Iino, 1990; Parker and Ivorra, 1990; Bezprozvanny *et al*., 1991; Finch *et al*., 1991). This provides the basis for an excitatory process allowing a Ca^{2+} wave to propagate by successive cycles of release, diffusion and Ca^{2+}-induced Ca^{2+} release (CICR) (Berridge and Dupont, 1994; Bootman *et al*., 1997a,b; Callamaras *et al*., 1998). Furthermore, a slower inhibitory process then terminates Ca^{2+} liberation during a wave and leads to a refractory state, from which the IP_3Rs must recover before a subsequent wave can arise (Iino, 1990; Parker and Ivorra, 1990; Bezprozvanny *et al*., 1991; Finch *et al*., 1991). A minimal model involving only the feedback regulation on IP_3Rs by cytosolic Ca^{2+} is, therefore, sufficient to account for the generation of repetitive Ca^{2+} oscillations (Hajnóczky and Thomas, 1997).

However, high-resolution Ca^{2+} imaging techniques have revealed that the cytoplasm does not act as a continuous, homogeneous excitable medium in which the generation of repetitive Ca^{2+} spikes can be explained in terms of the averaged population behavior of intracellular IP_3Rs. Instead, Ca^{2+} liberation occurs at discrete functional release sites, spaced a few micrometers apart, that generate localized, transient Ca^{2+} signaling events (Ca^{2+} 'puffs') involving the concerted opening of several, tightly clustered IP_3Rs (Parker and Yao, 1991; Yao *et al*., 1995; Berridge, 1997b; Bootman *et al*., 1997a,b; Sun *et al*. 1998; Thomas *et al*., 1998; Swillens *et al*., 1999). Ca^{2+} puffs function as 'building blocks' through which global Ca^{2+} waves propagate in a saltatory manner from release site to release site. Moreover, puffs arise autonomously before a wave is first initiated, and act as the triggers to initiate waves (Parker *et al*., 1996; Berridge, 1997b; Bootman *et al*., 1997b; Marchant *et al*., 1999).

The period between Ca^{2+} oscillations is, therefore, expected to be determined by two processes. First, the global sensitivity of IP_3Rs must recover from the refractory state resulting after one Ca^{2+} wave so that the overall excitability of the cytoplasm rises sufficiently so as to allow the active propagation of a subsequent wave. Secondly, an adequate local Ca^{2+} 'trigger' is then needed to initiate a wave. The distinction between these two requirements can be illustrated by analogy to the generation of cyclical forest fires. Following one fire, a second can not be sustained until the forest has re-grown sufficiently (recovery of IP_3R sensitivity). However, even after complete re-vegetation, a fire will not arise unless it is sparked by a sufficient triggering event such as a lightning strike (Ca^{2+} puffs). Furthermore, in addition to

these temporal considerations, which dictate the frequency of Ca^{2+} spiking, heterogeneity in properties and the subcellular distribution of puff sites determine the spatial patterning of Ca^{2+} signals. (Where is the fire sparked? What direction does it spread?) For example, Ca^{2+} waves repeatedly originate at specific subcellular regions in many cell types, including hepatocytes (Rooney *et al*., 1990; Thomas *et al*., 1996), pancreatic acinar cells (Kasai *et al*., 1993; Thorn *et al*., 1993) and neurons (Simpson *et al*., 1997).

We used *Xenopus* oocytes as a model system in which to assess the relative contributions of global and local processes in determining the periodicity and spatial organization of cellular Ca^{2+} signals. Specifically, we asked: (i) whether the wave period was determined simply by global recovery of cytosolic excitability, or by progressive changes in puffs that allowed them to serve as more effective triggers; and (ii) whether global Ca^{2+} waves were entrained by activity of particular puff sites. Repetitive Ca^{2+} oscillations were induced by sustained photorelease of IP_3, and were visualized, together with Ca^{2+} puffs, by real-time confocal microscopy. Our main findings are that the recovery of global excitability does not delimit solely the frequency of Ca^{2+} spiking, but that other mechanisms (including increases in puff frequency and amplitude, and accumulation of pacemaker Ca^{2+}) impart an additional latency before puffs are able to act as effective triggers to spark a wave. Furthermore, successive waves originate at particular 'focal' puff sites—distinguished by an intrinsically higher sensitivity to IP_3 and closer proximity to neighboring sites that amplify their activity—such that activity at these single elementary Ca^{2+} release sites can thereby entrain global cellular Ca^{2+} signals.

Results

Induction of repetitive Ca^{2+} waves by sustained photorelease of IP_3

Experiments were done using *Xenopus laevis* oocytes injected previously (30–120 min) with the Ca^{2+} indicator fluo-4 together with caged IP_3, to final intracellular concentrations of ~40 and 5 μM, respectively. Ca^{2+}-dependent fluorescence images were obtained at a rate of 15 frames/s (500 × 400 pixels) from a 65 × 65 μm region of the animal hemisphere of each oocyte, using a custom-built confocal scanner (Callamaras and Parker, 1999). UV light from an arc lamp was focused as a spot of ~200 μm diameter surrounding the scanned area, so that IP_3 could be photoreleased uniformly throughout the imaging frame. The UV light was turned on for long periods (10–30 min) at low intensity to produce a sustained photolysis, and the large volume of the oocyte (~1 μl) served as a reservoir so that the concentration of caged IP_3 did not become depleted appreciably during localized photolysis.

Figure 1 illustrates representative responses obtained using this protocol. The traces in Figure 1A show fluorescence measurements from two Ca^{2+} puff sites within the imaging field, and the images in Figure 1B show selected frames collected at corresponding times as marked in the fluorescence traces. The UV light was turned on at the beginning of the record, and was followed by a latent period of ~25 s during which little or no activity was observed. Individual Ca^{2+} puffs then arose independently at discrete sites (Figure 1Ba–c) and their frequency gradually increased until a puff at a particular site triggered a Ca^{2+} wave that propagated throughout the imaging field (Figure 1Bd–f). Following the wave, the overall Ca^{2+} level declined toward the baseline and activity ceased for a few seconds before puffs began to recur with gradually increasing frequency, leading eventually to the triggering of a subsequent wave (Figure 1Bg and h). This cycle repeated many times, and repetitive Ca^{2+} waves were evoked at a stable frequency for 20 min or longer (Figure 1C). We refer to the puff sites that initiated waves as 'focal' sites, and to other sites that showed puffs but failed to trigger waves as 'non-focal' sites. Successive waves in a train could arise at different focal sites but, as in Figure 1B, often arose repeatedly at specific foci.

The frequency of waves increases with increasing photorelease of IP_3 (Parker and Ivorra, 1993) and, by adjusting the intensity of the photolysis light, it was possible to evoke repetitive waves with interspike intervals varying from as short as 10 s to as long as 2 min (Figure 2A and B). At each photolysis intensity, the period remained stable for many cycles (Figure 2B). For example, the average variation in the interval between successive spikes in a train was only 18% of the mean (±1 SD; 33 oocytes from five frogs), indicating that a stable concentration of IP_3 was achieved after the first one or two spikes.

Occurrence of puffs between waves

Ca^{2+} puffs were silenced during, and shortly after a Ca^{2+} wave (Figure 1A and C), but then arose at increasing frequency throughout the interwave period until the next wave was triggered. To quantify the behavior of puffs during this period, we measured their frequencies and amplitudes at several sites (Figure 3). To normalize for differences in wave period between records, data are plotted as a function of wave phase, where a phase of '0' corresponds to the time of one wave peak and a phase of '–1' corresponds to the peak of the preceding wave. Furthermore, because the behavior of the puffs varied markedly with wave period, we separated the data into three groups (Figure 2B), corresponding to short- (<15 s), intermediate- (15–50 s) and long- (>50 s) period waves, evoked by differing intensities of photolysis light. At each of these periods, puffs were suppressed for ~7 s following a Ca^{2+} wave, after which activity gradually resumed. This suppression did not result artifactually from a failure to resolve puffs on a background of elevated Ca^{2+}, since puff activity was still absent several seconds after waves when the fluorescence had returned close to the baseline.

For short-period waves, almost no puffs were observed before a phase of '–0.5' (i.e. half way between one wave and the next), but their frequency then increased progressively before the next wave was triggered (Figure 3A). Overall, however, relatively few puffs arose prior to each wave (17 ± 7 events per 65 × 65 μm imaging field; mean ± 1 SD; n = 84 waves in 10 cells). During medium-period waves, puffs began again ~7 s following a Ca^{2+} wave (but, therefore, earlier in the phase cycle), and their frequency then increased steadily until the time of the subsequent wave (Figure 3C). Finally, during long-period

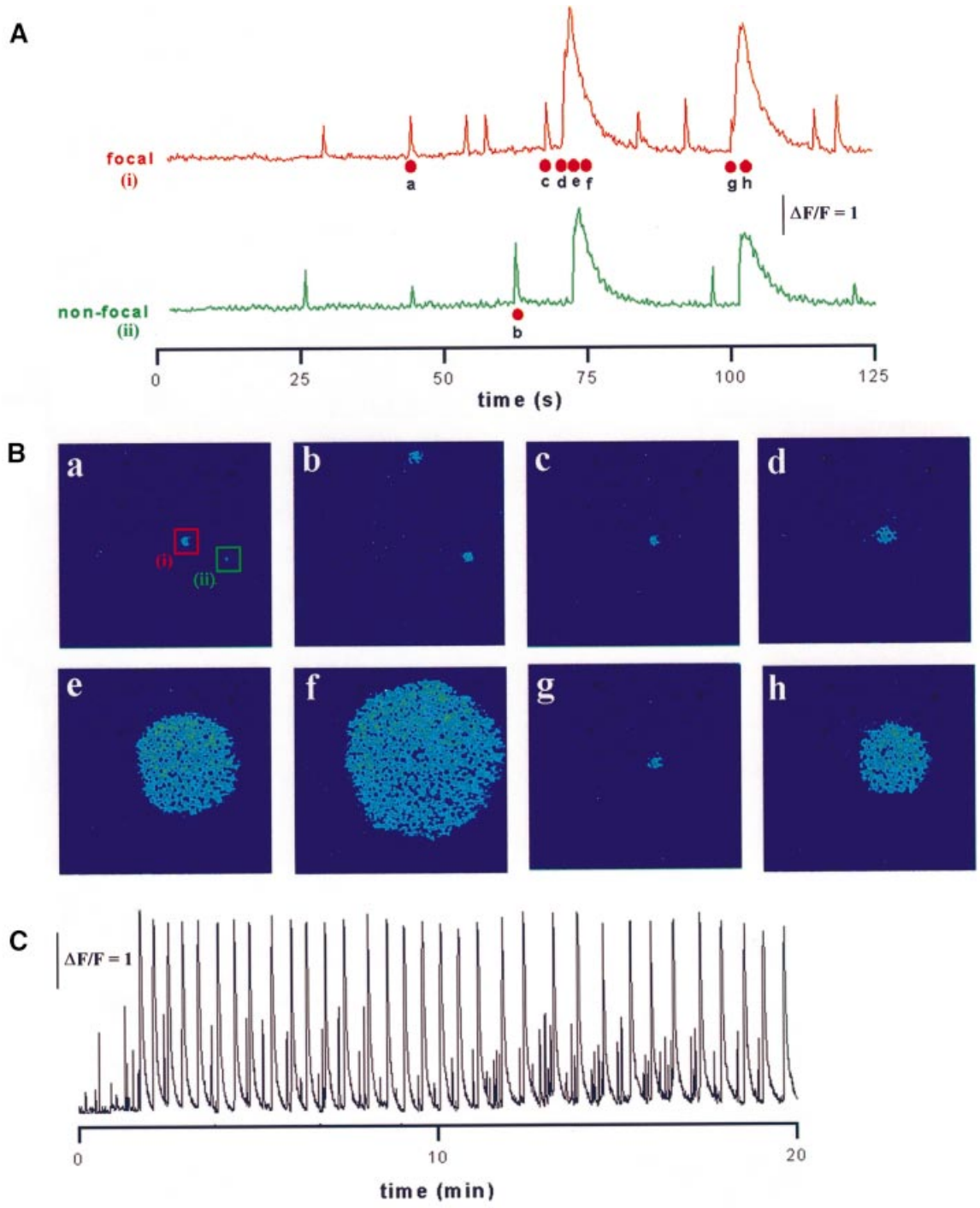

Fig. 1. Induction of puffs and periodic Ca^{2+} waves by sustained photorelease of IP_3. (**A**) Measurements of Ca^{2+}-dependent fluorescence monitored from 8 × 8 μm regions centered on two puff sites (i and ii) within the imaging field. The UV photolysis light was turned on at the start of the record, and remained on thereafter. Photoreleased IP_3 initially evoked asynchronous puffs at these sites (and at many other sites not shown), and a puff at site (i) triggered a Ca^{2+} wave that propagated throughout the imaging field. Puff activity ceased during the falling phase of the wave, but subsequently recovered until a second wave was again triggered by a puff at site (i). (**B**) Single image frames illustrating the spatial patterns of cytosolic Ca^{2+} observed at times corresponding to the points marked in (A). The sites from which the traces in (A) were obtained are marked on frame B (a). Panels depict Ca^{2+}-dependent fluorescence on a pseudo-color scale, after subtraction of resting fluorescence before stimulation. (**C**) Fluorescence trace from site (i) shown on a slower time scale illustrating periodic Ca^{2+} waves during sustained photolysis for 20 min.

waves, puffs appeared after an equally short delay (at a phase of '–0.9'), and their frequency increased to a sustained maximal level by about half way through the cycle (Figure 3E). The total number of puffs arising before each wave was thus much greater (114 ± 27 events per 65 × 65 μm imaging field; ±1 SD, n = 62 waves in eight cells) than during short-period waves.

In marked contrast to the increasing puff frequency through the wave cycle, the amplitudes of puffs showed little change (Figure 3B, D and F). Although puffs arising

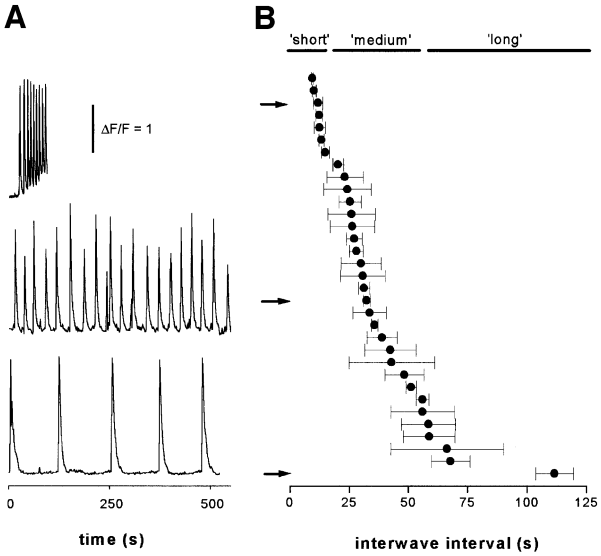

Fig. 2. Increasing photorelease of IP_3 evokes waves with progressively shorter periods. (**A**) Fluorescence traces (monitored from 8 × 8 μm boxes) from three different oocytes, exposed to UV light of constant intensity throughout each record. Repetitive waves with a mean period of ~10 s were evoked in the top record by relatively strong UV illumination, whereas the middle and lower traces show waves with periods of ~30 and ~110 s in response to progressively weaker stimuli. (**B**) The plot shows mean interwave intervals from 33 trials like those in (A), illustrating the range of periods explored. Error bars indicate 1 SD of the period derived from all successive waves during each trial. Arrows indicate data points corresponding to the traces in (A), and the bars show the arbitrary grouping of the data set into 'short'-, 'medium'- and 'long'-period records.

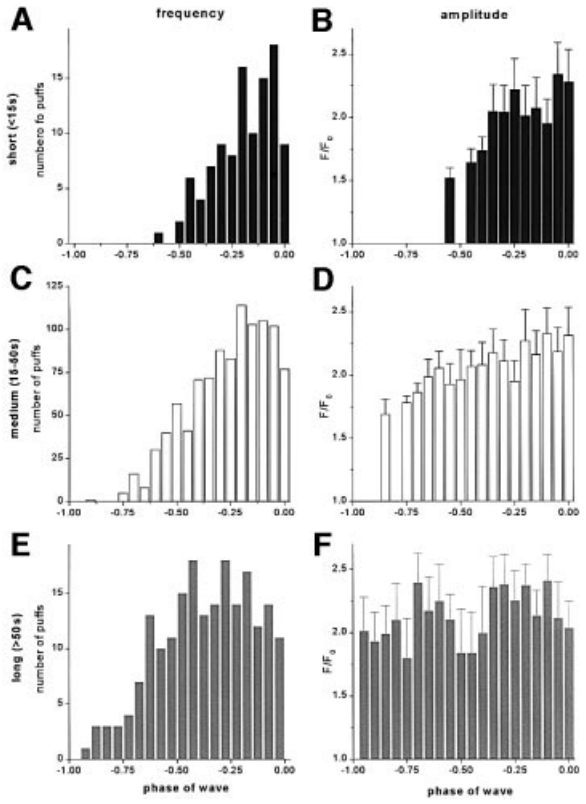

Fig. 3. Measurements of puff frequency and amplitude plotted as a function of phase of the wave cycle. Data are derived from the data set of Figure 2B, and were analyzed separately after grouping together records displaying waves with short (<15 s), medium (15–50 s) and long (>50 s) periods. (**A**, **C** and **E**) Histograms show the relative numbers of puffs observed throughout the entire imaging field (expressed as a percentage of the maximum) at different phases of the wave cycle. A phase of '0' corresponds to the peak of one wave, and a phase of '–1' to the peak of the preceding wave. (**B**, **D** and **F**) Corresponding histograms showing the distributions of peak fluorescence amplitudes (F/F_0) of these puffs.

very soon after a wave were slightly depressed, these represent only a small fraction of events, and the majority of puffs showed little or no systematic changes in amplitude during the interwave period.

Recovery of ability to support wave propagation

As described above, many puffs were observed between waves, particularly during long-period spiking. Two processes may be envisaged to account for the failure of these events to initiate waves. First, the ability of the cytoplasm to support wave propagation may recover slowly, so that the cell is refractory throughout most of the interwave period and can not be stimulated irrespective of the amount of trigger Ca^{2+}. Secondly, the ability of the cytoplasm to propagate waves may recover more rapidly but, even after it has become excitable, puffs may liberate insufficient Ca^{2+} to act as effective triggers (Marchant *et al*., 1999). To distinguish between these possibilities, we used a laser 'zap' technique (Marchant *et al*., 1999) to evoke large, localized Ca^{2+} elevations, so as to probe the excitability of the cytoplasm at different phases throughout the cycle of Ca^{2+} oscillations.

The protocol is illustrated in Figure 4A and B. Repetitive Ca^{2+} waves were induced by intracellular injection of the poorly metabolized IP_3 analog $I(2,4,5)P_3$, and several wave cycles were imaged to determine a regular periodicity. The oocyte was then stimulated by a brief (10 ms) exposure to an infrared laser, focused to a spot near the bottom left corner of the imaging field. This caused localized cell damage and generated a transient cytosolic Ca^{2+} elevation (Marchant *et al*., 1999). The laser intensity was adjusted to evoke Ca^{2+} transients considerably greater than individual puffs (Figure 4B,b and c). When delivered soon after a spontaneous wave, the laser zap evoked only a localized mobilization of Ca^{2+}, which diffused passively away from the stimulus site (Figure 4B). However, a zap delivered at a later phase in the wave cycle evoked a regenerative Ca^{2+} wave, which propagated throughout the imaging field (Figure 4A).

Figure 4C plots the probability that a laser zap would trigger a wave when applied at various phases during trains of repetitive Ca^{2+} spikes with periods of 15–30 s. The likelihood that the cell could sustain wave propagation was ~50% by half way through the wave cycle, and was 100% at wave phases greater than ~'0.7'. Therefore, the failure of the numerous puffs that occur during the later part of the wave cycle to trigger waves (Figure 3C) does not arise because the cell is inexcitable, but rather because individual puffs are ineffective stimuli for wave initiation.

Initiation of waves by puffs

The question then arises of what changes take place during the latter part of the wave cycle that finally allow a puff to trigger a wave, thereby determining wave periodicity. During short-period waves, a major factor is likely to be the recovery of IP_3Rs from a refractory state. Experiments

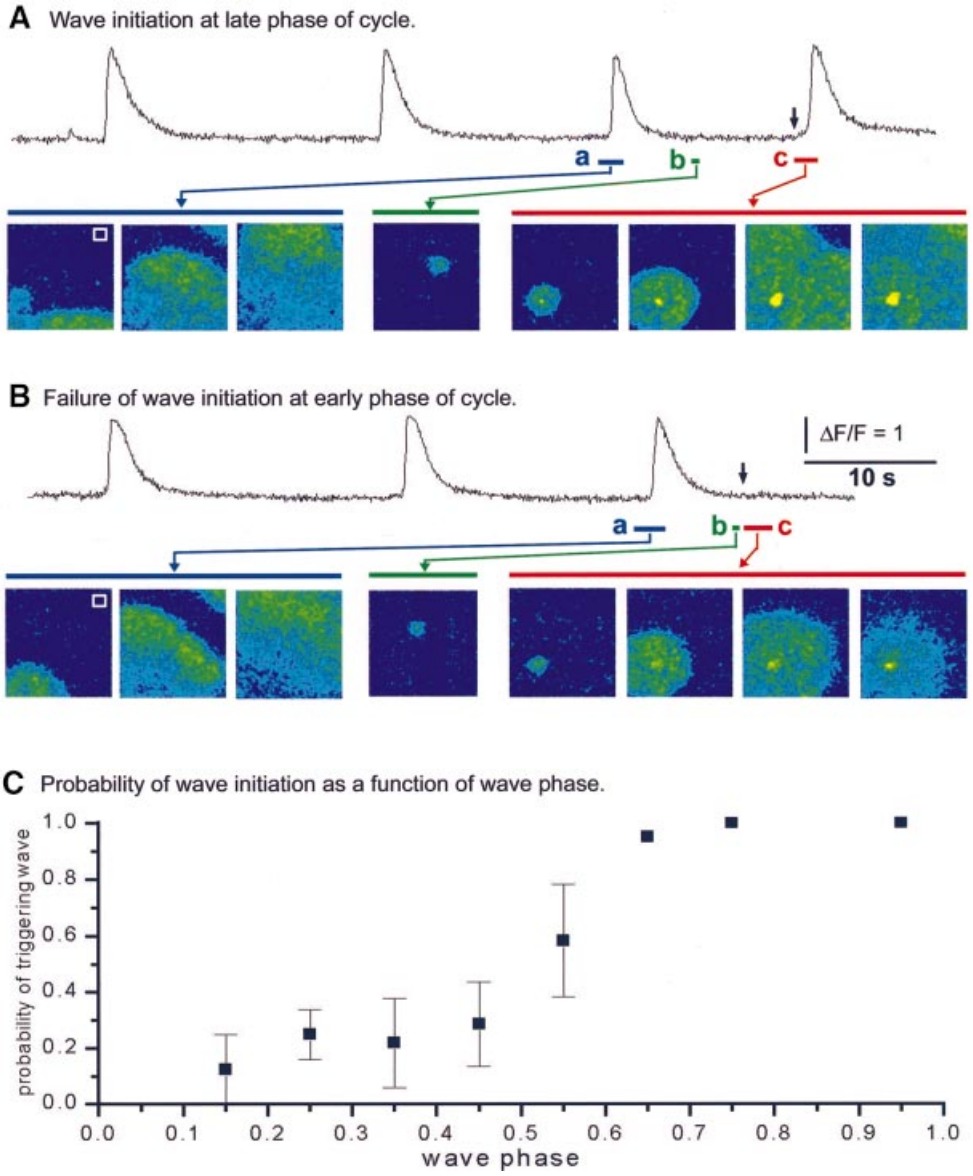

Fig. 4. The cytoplasm recovers the ability to propagate Ca^{2+} waves early during the wave cycle. (**A** and **B**) Experimental protocol using a laser 'zap' technique to probe the excitability of the cell. Repetitive Ca^{2+} waves were induced by injection of I(2,4,5)P_3. After recording three spontaneous waves, a laser pulse was delivered at various times so as to evoke a localized Ca^{2+} elevation near the bottom left corner of the imaging field. The traces in each section show fluorescence monitored near the top right corner of the field (white boxes), and the sequences of images show selected frames captured when indicated by the bars under the traces. Images illustrate (a) the propagation of periodic Ca^{2+} waves, (b) spontaneous Ca^{2+} puffs and (c) responses to a laser zap delivered when marked by the arrows above the traces. In (A), the laser zap was delivered relatively late during the wave cycle, and the local exogenous Ca^{2+} elevation triggered a Ca^{2+} wave that propagated throughout the imaging frame. In (B), the laser zap was delivered at an early phase during the wave cycle and failed to trigger a Ca^{2+} wave. (**C**) The plot shows the probability of triggering of Ca^{2+} waves by laser zaps delivered at varying phases throughout the wave cycle. Data were obtained from experiments like those in (A) and (B), from measurements during 57 trials (five oocytes) with wave periods of 15–30 s.

using paired photolysis flashes have shown that IP_3-evoked Ca^{2+} signals recover with a half-time of 3–4 s (Parker and Ivorra, 1990), so that the sensitivity of the cytosol would continue to increase further during the latter part of the wave phase after it had become capable of supporting wave propagation (Figure 4C). Furthermore, the puff frequency increased throughout the interwave period (Figure 3A), thus increasing the cumulative probability that an event would trigger a wave.

During long-period waves, on the other hand, neither of these mechanisms is likely to be significant. IP_3Rs would have recovered from their refractory state after >50 s, and the amplitudes and frequencies of puffs remained constant during the latter half of the wave cycle (Figure 3E and F). Instead, a slow accumulation of cytosolic Ca^{2+} resulting from puff activity may sensitize release sites during periodic waves, in the same way as before initial wave activation (Bootman *et al*., 1997b; Marchant *et al*., 1999), so that the amount of Ca^{2+} liberated by a puff becomes sufficient to initiate wave propagation. Figure 5 shows measurements of basal Ca^{2+} fluorescence during short- (<15 s) and long- (>50 s) period waves, plotted for comparison together with corresponding measurements of puff frequency. The basal Ca^{2+} level declined

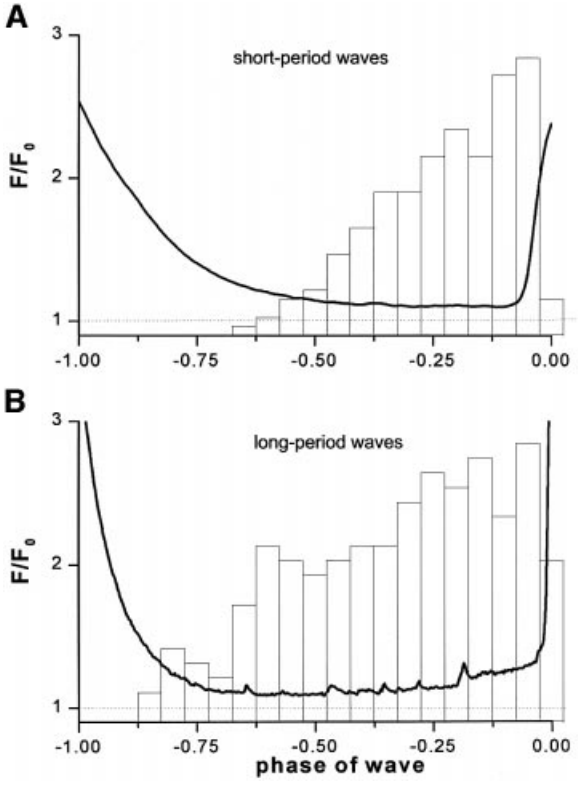

Fig. 5. The basal Ca^{2+} level around focal sites increases slowly before each wave during long-period spiking, but not during short-period spiking. (**A**) The solid trace shows the basal Ca^{2+} fluorescence signal in the vicinity of focal puff sites as a function of wave phase for short-period (<15 s) waves. This is an average from 32 sites, obtained by measuring the mean fluorescence ratio within 8 × 8 μm regions centered on focal puff sites. A ratio of $F/F_0 = 1$ (dashed line) corresponds to the resting Ca^{2+} level before photorelease of IP_3. The superimposed histogram shows, for comparison, the corresponding increase in puff frequency, replotted from Figure 3A and aligned to the time of wave initiation. (**B**) Similar data obtained during long-period (>50 s) waves.

progressively between waves with short periods (Figure 5A). In contrast, the Ca^{2+} level during long-period waves declined to a minimum about one-third of the way through the wave cycle and then increased, presumably reflecting a balance between the accumulation of Ca^{2+} liberated into the cytosol by puffs and its subsequent re-sequestration (Figure 5B). Sensitization of IP_3Rs by a pacemaker elevation of basal [Ca^{2+}] may thus play an important role in wave triggering during long-period spiking, but is not a significant mechanism at short periods.

Specific puff sites serve as foci for repetitive wave initiation

Ca^{2+} puffs arose at discrete sites, which remained at fixed positions in the cell throughout records as long as 30 min. On average, 39 sites were evident within the imaging field of 65 × 65 μm (1288 sites in 33 records), corresponding to a density of ~1 site per 100 μm^2.

An important observation was that most puff sites never acted as foci to initiate waves. Instead, a single site or a few sites acted repeatedly to initiate successive Ca^{2+} waves, as illustrated in Figure 6A, where nine sequential waves originated at a single focus, even though 59 other non-focal puff sites were present in the imaging field.

To determine whether the appearance of such 'eager' focal sites might arise through statistical variation, we compared experimental data with those expected if all puff sites had an equal probability of initiating a wave. Experimental data (open bars, Figure 6B), derived from 33 imaging sites each displaying trains of 10 waves with periods of 9–110 s, showed relatively few (76/330) instances where a site initiated only one wave, but many instances where a given site triggered 4–10 waves. In marked contrast, a simulation of the same protocol (33 trains with 10 waves per train) in which all puff sites were equivalent predicted that most waves (276/330) would initiate at different sites during each train, and that no instances would be expected where four or more waves in a train originated at the same focus.

The ability of particular sites to initiate multiple waves was most prominent during long-period spiking. The mean percentage of puff sites that acted as foci to initiate one or more waves was 12 ± 3% for short-period waves (<15 s; 70 waves), as compared with 7 ± 1% for medium-period waves (15–50 s; 180 waves) and 3 ± 1% for long-period waves (>50 s; 80 waves).

A trivial explanation for the ability of particular sites to initiate multiple waves could be that the photorelease of IP_3 was inhomogeneous so that, for example, a higher intensity of UV light in the center of the imaging field led to a higher local activation of puff sites in that region. This possibility can be excluded because both focal and non-focal puff sites showed a relatively uniform distribution throughout the imaging field (Figure 6C).

Magnitude and kinetics of Ca^{2+} signals are similar at focal and non-focal sites

One explanation for the preferential ability of focal sites to initiate waves might be that they generate larger or more prolonged puffs, thus providing a greater amount of trigger Ca^{2+}. Figure 7A shows the distributions of peak fluorescence amplitudes (F/F_0) of puffs at focal and non-focal sites. No appreciable differences were apparent between these distributions, nor in the mean puff amplitudes (focal sites, $F/F_0 = 1.49 \pm 0.04$, 1100 events in 15 oocytes; non-focal sites, $F/F_0 = 1.46 \pm 0.07$, 350 events, 15 oocytes). Furthermore, the spatial spread of Ca^{2+} signals at focal and non-focal sites was similar (Figure 7B; mean full-width at half-maximal amplitude 6.4 ± 1.4 μm focal, 14 sites; 7.0 ± 1.6 μm non-focal, 18 sites), as were the half-decay times of puffs (Figure 6C; 389 ± 41 ms focal, 14 sites; 488 ± 74ms non-focal, 18 sites).

Focal sites are located close to their neighbors and display a high frequency of puffs

Given that puffs at focal sites are no larger or more prolonged than puffs at non-focal sites, we looked for other distinguishing properties of focal sites. One characteristic is that focal sites were located more closely to neighboring puff sites, thereby enhancing their ability to initiate a wave by CICR. Figure 8 shows a scatter plot of nearest-neighbor distributions around focal (filled symbols) and non-focal sites (open symbols), derived from 33 records of repetitive waves with periods of 10–110 s. The mean separation of focal sites from their nearest

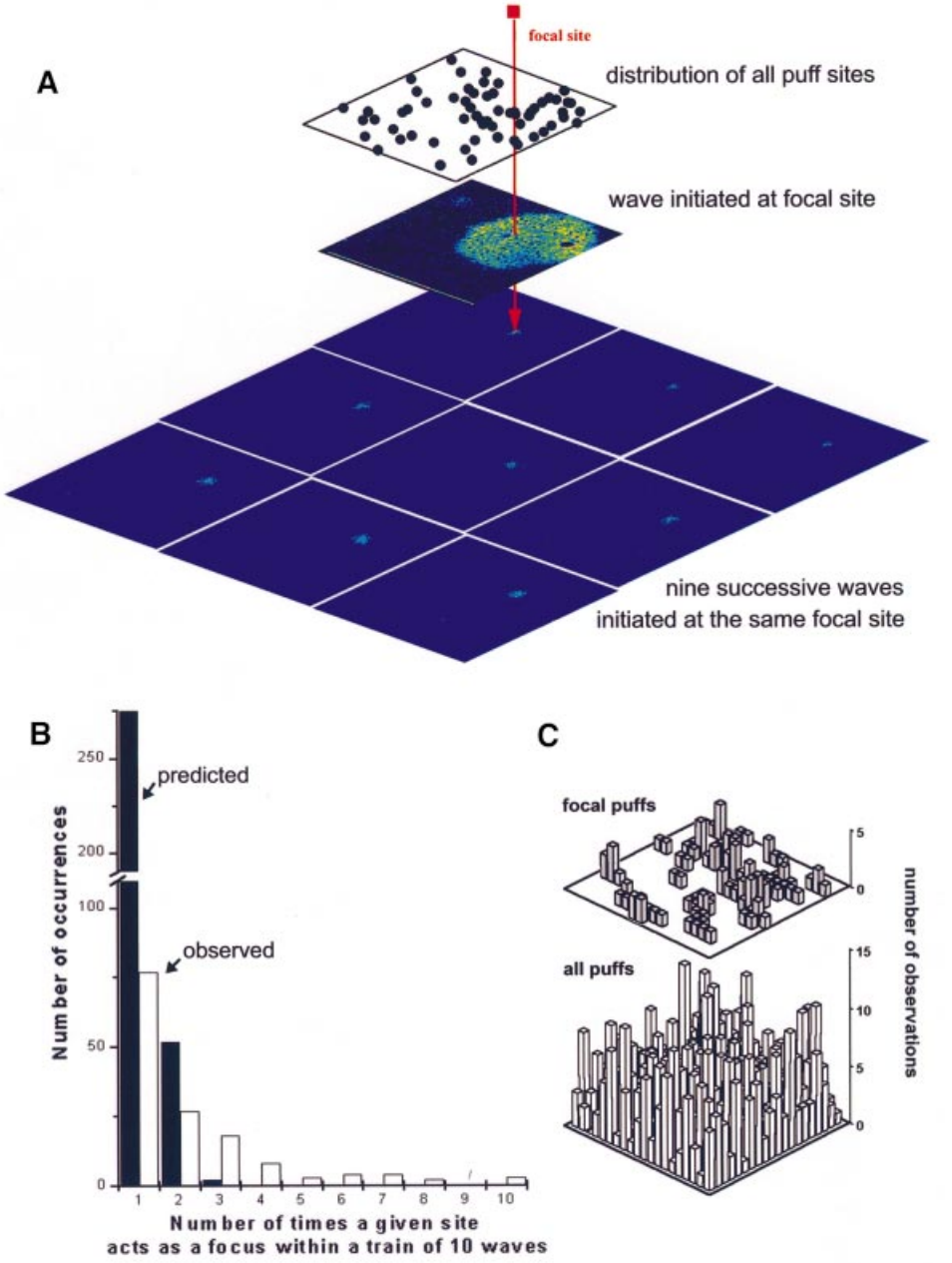

Fig. 6. Waves are triggered preferentially at specific, focal puff sites. (**A**) Images illustrating the initiation of nine successive Ca^{2+} waves (period ~50 s) at a single, focal puff site. The upper panel shows the distribution of all 58 puff sites observed throughout the imaging field during a 35 min record. The middle panel shows a circular wave that originated at the focal site marked in red. The lower mosaic of nine panels shows images captured at the beginning of nine successive waves, that all originated at the same site. (**B**) Experimental (open bars) and predicted (solid bars) distributions of occurrences where *n* (1, 2, 3, etc.) waves out of a train of 10 arose at a given site. Experimental data were obtained from 33 records, measuring the first 10 waves in each train (i.e. 330 waves in total). The mean number of puff sites within the imaging field was 40 (1288 sites in 33 records). The predicted distribution was obtained assuming 40 puff sites per field, which all had an equal probability of wave initiation. To simulate this situation, we generated 33 sequences of 10 random integer numbers within the range 1–40, and counted the numbers of occurrences where a given integer (corresponding to a particular site puff site) arose *n* times within each set of 10. (**C**) Focal and non-focal puffs sites are located randomly throughout the imaging field. Plots show distributions of focal (top) and non-focal (bottom) puff sites within a 65 × 65 μm imaging plane, scored by position within a grid of individual ~10 μm^2 regions. Measurements were made in 33 oocytes, from records such as those shown in (A).

neighbors was 4.9 ± 0.2 μm (141 sites), as compared with 7.3 ± 0.3 μm for non-focal sites (n = 168).

A further distinguishing feature of focal sites was that they displayed a higher frequency of puffs. The mean number of puffs per focal site in records with Ca^{2+} wave periods between 10 and 110 s was 140 ± 10% of that at non-focal sites (n = 146 focal sites, 673 non-focal sites; 33 oocytes), and this difference became more pronounced (167 ± 18%) when analysis was restricted to those focal sites (n = 33) that initiated more than one wave in each record.

Focal sites display higher sensitivity to IP_3

The higher frequency of puffs at focal sites suggested that these sites have a higher sensitivity to IP_3. However, localized differences in basal free Ca^{2+}

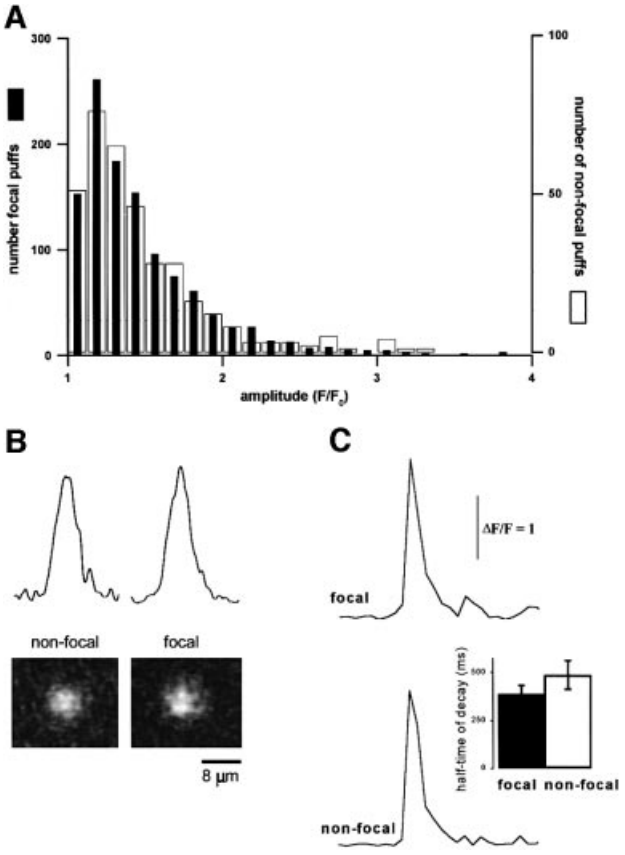

Fig. 7. Puffs at focal sites display similar amplitudes and kinetics to those at non-focal sites. (**A**) Histograms show distributions of peak puff amplitudes at focal (filled bars) and non-focal (open bars) sites. Measurements were made as peak fluorescence ratio (F/F_0) measured within an 8 × 8 µm box centered at puff sites. Data (1100 focal events, 350 non-focal events; 33 oocytes) were obtained during repetitive waves with periods of 10–110 s. Puffs that directly triggered waves were excluded. Representative non-focal sites were selected using a random number generator. (**B**) The spatial spread of puffs is similar at focal and non-focal sites. Images show averaged puffs at focal (n = 14) and non-focal (n = 18) sites, formed by capturing individual frames at the time of maximal puff amplitude averaging after spatially aligning their centers. Traces show corresponding fluorescence profiles measured along a line (3 pixel width) passing diametrically through the centers of the averaged events. (**C**) Puffs at focal and non-focal sites show similar decay times. Traces show kinetics of fluorescence signals measured from 8 × 8 pixel boxes centered on focal and non-focal puff sites. Records are averages of 14 focal and 18 non-focal events. The histogram plots the mean half-time for decay of fluorescence at focal (n = 14) and non-focal sites (n = 18).

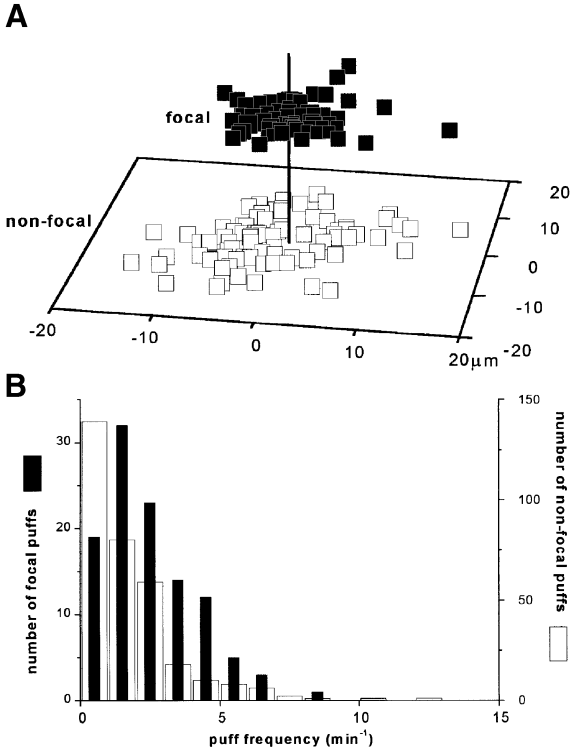

Fig. 8. Focal sites are located closer to neighboring sites than are non-focal sites, and exhibit a higher frequency of puffs. (**A**) The scatter plot shows the locations of the nearest neighboring puff site with respect to selected focal sites (filled squares, n = 141) and randomly selected non-focal sites (open squares, n = 168). The plot was generated by aligning each selected site (focal or non-focal) at the center of the field (vertical line) and then mapping the position of the nearest neighboring puff site. (**B**) Distribution of puff frequencies at focal (filled bars; left axis) and non-focal (open bars; right axis) puff sites. Data were obtained from 33 records (five frogs).

concentration could also contribute to this effect. To separate these factors, we loaded oocytes with the slow Ca^{2+} buffer EGTA, so as to disrupt CICR resulting from Ca^{2+} diffusing between release sites, thereby functionally uncoupling individual sites (Figure 9A: Callamaras and Parker, 2000).

The locations of focal and non-focal puff sites were first mapped by sustained photorelease of IP_3 to evoke Ca^{2+} oscillations in the usual way. EGTA was then microinjected to a final intracellular concentration of ~300 µM during continued photolysis. Repetitive waves ceased shortly after EGTA loading, but puffs continued to arise at the same locations with little diminution in amplitude or frequency (Figure 9B). The frequency of puffs before loading EGTA was higher at focal sites than at non-focal sites (3.8 versus 2.8 puffs/min; 26 paired sites, 10 oocytes). This difference was maintained after injection of EGTA (3.8 versus 2.4 puffs/min), suggesting that Ca^{2+} sensitization between closely coupled sites was not solely responsible for the higher puff frequency at focal sites.

The relative sensitivities of different sites to IP_3 were assessed using weak photolysis flashes that evoked puffs with low probability. Focal sites displayed a higher probability of generating puffs than did randomly selected non-focal sites (Figure 9E): 52.5 ± 5.8% of focal sites gave at least one puff during 10 successive flashes, compared with 34.7 ± 3.3% of non-focal sites (n = 597 sites from 10 imaging fields in 10 oocytes). Furthermore, focal puff sites responded more often (2.7 ± 0.4 puffs per 10 flashes; 20 sites) than non-focal sites (1.5 ± 0.1 puffs per 10 flashes from sites that responded at least once). This difference was enhanced further when comparison was restricted to those focal sites that triggered multiple waves prior to injection of EGTA (Figure 9F; 3.7 ± 0.5 puffs per 10 flashes, n = 10 sites versus 0.5 puffs at all non-focal sites), indicating that the most active focal sites display an intrinsic sensitivity to IP_3 ~7-fold greater than non-focal sites.

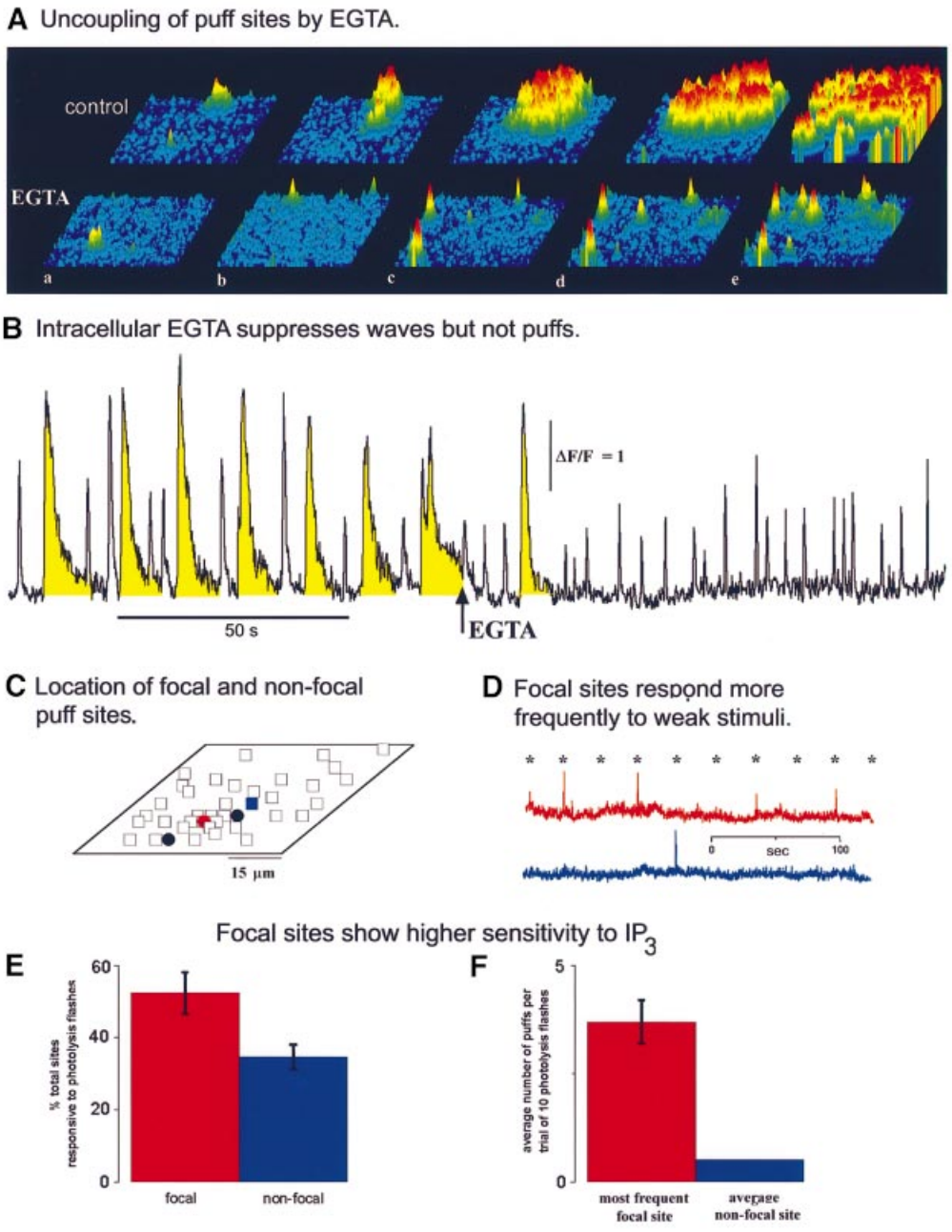

Fig. 9. Focal wave initiation sites display an intrinsically higher sensitivity to IP_3. (**A**) Image sequences illustrating the functional uncoupling of puff sites following intracellular loading of the slow Ca^{2+} buffer EGTA. Each image sequence (a–e) was captured at intervals of 100 ms, and illustrates the patterns of Ca^{2+} liberation evoked in an oocyte by a photolysis flash of fixed intensity before (top) and after (bottom) loading EGTA to a final intracellular concentration of ~300 μM. The flash evoked a propagating Ca^{2+} wave in control conditions, but gave only discrete puffs after loading EGTA. Records were obtained from a 65 μm^2 region of the animal hemisphere, in response to photolysis flashes delivered just before the image sequences. (**B**) Abolition of Ca^{2+} waves by EGTA. Fluorescence signals were measured from an 8 μm^2 region centered on a puff site in response to sustained photorelease of IP_3 throughout the entire record. Repetitive Ca^{2+} waves (highlighted in yellow) and puffs were evoked in control conditions. The waves were abolished rapidly following injection of EGTA (arrowed), but puffs continued with little change in amplitude or frequency. (**C**) Schematic diagram, illustrating the protocol for measuring the relative sensitivities of puff sites. The locations of focal (filled circles) and non-focal puff sites (open squares) within the 65 μm^2 imaging plane were mapped during sustained photorelease of IP_3 as in (B). EGTA was then injected, and responses were monitored from the same puff sites in response to weak photolysis flashes. (**D**) The traces show puffs evoked at representative focal and non-focal sites (marked in C by the red circle and blue square, respectively), in response to a train of 10 photolysis flashes delivered at 30 s intervals as marked by the asterisks. (**E**) Percentages of focal sites (red) and non-focal sites (blue) that gave one or more puffs during a train of 10 photolysis flashes. (**F**) Average numbers of puffs evoked per 10 flashes at frequent focal puff sites (red) and representative non-focal sites (blue).

Discussion

The clustered arrangement of IP_3Rs in the cytoplasm permits two modes of Ca^{2+} signaling: local Ca^{2+} puffs where CICR is restricted to individual release sites, and global Ca^{2+} waves that propagate in a saltatory manner between sites (Parker *et al*., 1996; Berridge, 1997b; Bootman *et al*., 1997b). We previously investigated the transition between local and global Ca^{2+} signaling when $[IP_3]$ was elevated initially, and demonstrated that both

modes of signaling can co-exist in *Xenopus* oocytes, because the amount of Ca^{2+} liberated by a puff is usually below the threshold for wave initiation (Marchant *et al*., 1999). The present study extends those studies to examine the role of puffs during repetitive Ca^{2+} waves generated by sustained photorelease of IP_3. This represents a mechanistically different case, as during Ca^{2+} oscillations the wave interval is determined both by recovery of global excitability from a refractory state and by progressive changes in puff behavior.

Factors determining wave period

The generation of each successive Ca^{2+} wave in a train requires that two distinct conditions be met. First, the overall excitability of the cytoplasm must recover sufficiently from the inactivation induced by the previous wave so that the next wave can propagate. Secondly, a trigger is needed to initiate that wave. By using laser stimulation to evoke local Ca^{2+} elevations much larger than puffs, we show that Ca^{2+} waves could be evoked reliably during the latter third of the wave cycle (Figure 4). Irrespective of the wave period, puffs were suppressed for only ~7 s following a wave, but then occurred in increasing numbers before the next wave. Therefore, even though the cell was capable of supporting waves, numerous puffs arose without triggering a wave (Figure 3), indicating that the duration of the interwave interval is set neither by the time required for the cytoplasm to recover its ability to support wave propagation, nor by the interval until the first puffs reappear.

The likelihood that a puff will initiate a wave depends upon the amount of Ca^{2+} released relative to the threshold amount required to evoke CICR from neighboring sites (Marchant *et al*., 1999). During short-period (<15 s) waves, at least three mechanisms may contribute toward a progressive increase in this ratio during the latter part of the wave cycle: (i) the recovery of IP_3Rs from inactivation (half time of ~4 s; Parker and Ivorra, 1990) progressively reduces the threshold Ca^{2+} required for wave initiation; (ii) puff amplitudes increase, making them more effective triggers; (iii) puff frequency increases, increasing the cumulative likelihood of wave triggering.

On the other hand, none of these processes appears to be significant in determining the periodicity of slow (>50 s) waves. At these intervals, recovery of IP_3Rs is expected to be substantially complete early during the wave phase, and puffs arose with constant frequency and amplitudes throughout the latter half of the wave cycle. Instead, the accumulation of Ca^{2+} liberated during puffs leads to a pacemaker rise of overall cytosolic [Ca^{2+}], which sensitizes CICR and thereby facilitates the ability of a puff to initiate a wave (Iino *et al*., 1993; Bootman *et al*., 1997b; Marchant *et al*., 1999). This pacemaker Ca^{2+} signal was apparent only between long-period waves, and points to the particular importance of factors that influence Ca^{2+} handling, including sequestration into the ER (Camacho and Lechleiter, 1993; Pozzan *et al*., 1994) and mitochondria (Jouaville *et al*., 1995; Simpson *et al*., 1997; Rizzuto *et al*., 1999) as well as Ca^{2+} influx across the cell membrane (Yao and Parker, 1994; Berridge and Dupont, 1994; Berridge 1997b), in modulating the frequency of long-period waves.

The occurrence of puffs at any given site is stochastic, so that intervals between events at that site are highly variable (Yao *et al*., 1995). Despite this, repetitive Ca^{2+} waves triggered by puffs showed a regular periodicity at any given [IP_3]. This apparent discrepancy can be explained because wave initiation results largely from the summated behavior of numerous puff sites—a chemical mechanism analogous to the summation of stochastic single-channel openings to provide reproducible macroscopic whole-cell currents. Nevertheless, the numerous puffs that arise between waves may serve a signaling function in their own right. Whereas subcellular regions close to puff sites experience transient elevations of free Ca^{2+} concentration of similar magnitude whether that site generates a puff or is activated during a wave (Callamaras *et al*., 1998), more distant regions experience appreciable Ca^{2+} signals only during Ca^{2+} waves. Thus, Ca^{2+}-dependent processes located close to puff sites that are active between waves will experience a net frequency of local Ca^{2+} spikes several fold higher than the global cellular periodicity.

Focal wave initiation sites

Although Ca^{2+} oscillations were driven by the aggregate activity of puffs, the behavior of individual puff sites within this population was not equivalent; rather, repetitive waves during long-period (>50 s) oscillations repeatedly initiated at preferred 'focal' puff sites (Figure 6; Lechleiter *et al*., 1991). This is unlikely to arise simply through an immediacy effect (whereby the first site to generate a wave is the first to recover from inactivation), because all sites throughout the imaging field were recruited by a wave within <2 s, whereas focal entrainment was most apparent during waves with much longer periods (up to 120 s). Furthermore, no differences were apparent in amplitude, spatial spread or kinetics of puffs between focal and non-focal sites, indicating that focal sites do not release more Ca^{2+} (Figure 7). However, focal sites displayed a higher frequency of puffs and were located closer to neighboring sites (Figure 8). By using the slow Ca^{2+} buffer EGTA to functionally uncouple puff sites (Callamaras and Parker, 2000), we show that focal puff sites have an intrinsically higher sensitivity to IP_3 than non-focal sites (Figure 9). This will strongly influence the location of wave initiation, because even small differences in sensitivity are highly magnified by the regenerative feedback of CICR. The higher sensitivity to IP_3 will result in a higher puff frequency at focal sites, accentuating the local accumulation of pacemaker Ca^{2+} and hence the cumulative probability that a puff will trigger a wave. Furthermore, neighboring sites will experience a strong Ca^{2+} sensitization by virtue of their close proximity to a focal site, and will be more likely to be triggered by CICR to set in motion the regenerative process that begins a wave.

We note, however, that entrainment of waves by focal sites was not absolute and, even during long-period spiking, waves often initiated alternately at a few different focal sites. In particular, a wave began at a new site within seconds after an established focal site was rendered temporarily inexcitable by generating an abortive wave. However, the *Xenopus* oocyte is atypical of most cells in at least two aspects: first, it is a giant cell possessing an

enormous number of puff sites; secondly, puffs are generated by clusters containing only a single IP_3R isoform (Parys and Bezprozvanny, 1995), with most sites displaying similar sensitivities to IP_3 (Yao *et al*., 1995; Parker *et al*., 1996). Both factors will minimize the ability of specific sites to dominate global Ca^{2+} signaling. The situation may be very different in other cells expressing IP_3R isoforms with differing IP_3 affinities (Newton *et al*., 1994), where entrainment of global Ca^{2+} signals by a single puff site is more pronounced (Thomas *et al*., 2000), and may be important both for determining the temporal periodicity of Ca^{2+} waves and for imposing their spatial vector (i.e. where waves begin and in what direction they travel). Temporal entrainment is exemplified by the HeLa cell, which contains only a handful of puff sites from which a single 'pacemaker' site dominates wave initiation (Bootman *et al*., 1997a, b; Thomas *et al*., 2000). Vectorial entrainment is exemplified by the pancreatic acinar cell, where Ca^{2+} waves originate within the secretory pole from regions of high IP_3 sensitivity (Kasai *et al*., 1993; Thorn *et al*., 1993) that overlap with the distribution of the higher affinity type II IP_3Rs (Lee *et al*., 1997).

A final point concerns the molecular basis underlying the enhanced sensitivity of focal puff sites. Our experiments indicate that this does not arise through spatial gradients of $[IP_3]$ (uniform photorelease) or cytosolic free $[Ca^{2+}]$ (clamping with EGTA). Further, the oocyte lacks the heterogeneity of IP_3R subtypes that generates differing IP_3 sensitivities in other cells (Parys and Bezprozvanny, 1995). It is unlikely that focal sites contain a greater number of IP_3Rs, because the amounts of Ca^{2+} liberated by focal and non-focal puffs were similar, although enhanced sensitivity might result if these receptors were more closely packed in the cluster. Other possibilities include modulation of the tonic sensitivity of IP_3Rs by differential phosphorylation, binding of accessory proteins, or luminal $[Ca^{2+}]$ gradients. Although our data indicate that the locations of focal sites remain constant for several minutes, an intriguing possibility is that the sensitivity of focal sites could be regulated dynamically over longer periods, providing cells with great flexibility in modulating the frequency and directionality of global Ca^{2+} signals.

Materials and methods

Experiments were performed on stage V and VI oocytes obtained from *X.laevis* as described previously (Marchant *et al*., 1999). Frogs were anesthetized by immersion in a 0.15% aqueous solution of MS-222 (3-aminobenzoic acid ethyl ester) for 15 min, and pieces of ovary were removed surgically. Epithelial layers were removed either manually or by collagenase treatment (Sigma Type I, used at 1 mg/ml for 1 h), and oocytes were microinjected 1 h prior to recording with the Ca^{2+} indicator fluo-4 together with caged IP_3 [*myo*-inositol 1,4,5-trisphosphate, $P^{4(5)}$-1-(2-nitrophenyl) ethyl ester], to final intracellular concentrations of ~40 and ~5 μM, respectively. Recordings were made at room temperature, imaging in the animal hemisphere of oocytes bathed in Ringer's solution (120 mM NaCl, 2 mM KCl, 1.8 mM $CaCl_2$, 5 mM HEPES pH 7.2). Fluo-4 and caged IP_3 were obtained from Molecular Probes Inc. (Eugene, OR). All other reagents were from Sigma Chemical Co. (St Louis, MO).

Ca^{2+} imaging was performed using a custom-built confocal scanner interfaced to an Olympus IX50 inverted microscope equipped with a 40× oil-immersion objective (Callamaras and Parker, 1999). In brief, fluorescence was excited by the 488 nm beam from an argon-ion laser and emitted light was detected through a confocal pinhole, providing an optical section of ~0.8 μm. The laser spot was scanned by a resonant mirror to provide 'real-time' *x–y* imaging of a 450 × 450 pixel frame every 66 ms. Fluorescence images were obtained with the microscope focused at the level of the pigment granules in the oocyte (where Ca^{2+} release sites are concentrated; Callamaras and Parker, 1999) and are expressed as a pseudoratio (F/F_0) of the intensity at each pixel (F) relative to that at the same pixel before stimulation (F_0). IP_3 was photoreleased by irradiation with UV light from a mercury arc lamp, focused uniformly throughout a 200 μm diameter spot surrounding the imaging frame. The light intensity was varied by neutral density filters to regulate the rate of photorelease of IP_3. Video data were recorded on digital tape for subsequent processing and analysis using MetaMorph (Universal Imaging, Westchester, PA) and IDL (Research Systems Inc., Boulder, CO) software packages. Data are presented as mean ± 1 SEM unless otherwise indicated.

Experiments employing a laser 'zap' technique to evoke focal Ca^{2+} elevations (Figure 4) were done using the same confocal imaging system, except that the epifluorescence port of the microscope was switched to allow introduction of a near infrared laser beam. The principle of this method is to cause energy absorption by pigment granules in the oocyte, leading to local 'photoperforation' and transient mobilization of Ca^{2+} from intra- and extracellular sources (Marchant *et al*., 1999). Laser light (780 nm) was derived from a Ti-sapphire laser (Tsunami; Spectra Physics, CA) operated in continuous wave mode, and was focused as a spot near one corner of the imaging field. Pulses of 10 ms duration (set by an electromechanical shutter) were delivered at varying phases during repetitive Ca^{2+} waves induced by the non-metabolizable IP_3 analog $I(2,4,5)P_3$ at final intracellular concentrations of 20–100 nM. This system differs from our previous procedure (Marchant *et al*., 1999) in using an infrared, rather than a pulsed UV laser, and by evoking Ca^{2+} waves by use of a non-metabolizable IP_3 analog rather than by photolysis of caged IP_3. These changes were imposed by the optical arrangement of our present microscope; however, the principle of the laser zap technique remains unchanged.

Acknowledgements

This work was supported by grants GM 48071 (NIH) and by a Wellcome Trust Fellowship (053102) to J.S.M.

References

Berridge,M.J. (1997a) The AM and FM of calcium signalling. *Nature*, **386**, 759–760.

Berridge,M.J. (1997b) Elementary and global aspects of calcium signalling. *J. Physiol.*, **499**, 291–306.

Berridge,M.J. and Dupont,G. (1994) Spatial and temporal signalling by calcium. *Curr. Opin. Cell Biol.*, **6**, 267–274.

Bezprozvanny,I., Watras,J. and Ehrlich,B.E. (1991) Bell-shaped calcium-response curves for $Ins(1,4,5)P_3$- and calcium-gated channels from endoplasmic reticulum of cerebellum. *Nature*, **351**, 751–754.

Bootman,M.D., Niggli,E., Berridge,M.J. and Lipp,P. (1997a) Imaging the hierarchical Ca^{2+} signalling system in HeLa cells. *J. Physiol.*, **499**, 307–314.

Bootman,M.D., Berridge,M.J. and Lipp,P. (1997b) Cooking with calcium; the recipes for composing global signals from elementary events. *Cell*, **91**, 367–373.

Callamaras,N. and Parker,I. (1999) Construction of a confocal microscope for real-time *x–y* and *x–z* imaging. *Cell Calcium*, **26**, 271–280.

Callamaras,N. and Parker,I. (2000) Phasic characteristic of elementary Ca^{2+} release sites underlies quantal responses to IP_3. *EMBO J.*, **19**, 3608–3617.

Callamaras,N., Marchant,J.S., Sun,X.-P. and Parker,I. (1998) Activation and coordination of $InsP_3$-mediated elementary Ca^{2+} events during global Ca^{2+} signals in *Xenopus* oocytes. *J. Physiol.*, **509**, 81–89.

Camacho,P. and Lechleiter,J.D. (1993) Increased frequency of calcium waves in *Xenopus laevis* oocytes that express a calcium-ATPase. *Science*, **260**, 226–229.

Dal Santo,P., Logan,M.A., Chisholm,A.D. and Jorgensen,E.M. (1999) The inositol trisphosphate receptor regulates a 50-second behavioral rhythm in *C. elegans*. *Cell*, **98**, 757–767.

De Koninck,P. and Schulman,H. (1998) Sensitivity of CaM kinase II to the frequency of Ca^{2+} oscillations. *Science*, **279**, 227–230.

Dolmetsch,R.E., Lewis,R.S., Goodnow,C.C. and Healy,J.I. (1997) Differential activation of transcription factors induced by Ca^{2+} response amplitude and duration. *Nature*, **386**, 855–858.

Fewtrell,C. (1993) Ca^{2+} oscillations in non-excitable cells. *Annu. Rev. Physiol.*, **55**, 427–454.

Finch,E.A., Turner,T.J. and Goldin,S.M. (1991) Calcium as a coagonist of inositol 1,4,5-trisphosphate-induced calcium release. *Science*, **252**, 443–446.

Hajnóczky,G. and Thomas,A.P. (1997) Minimal requirements for calcium oscillations driven by the IP_3 receptor. *EMBO J.*, **16**, 3533–3543.

Iino,M. (1990) Biphasic Ca^{2+}-dependence of inositol 1,4,5-trisphosphate-induced Ca^{2+} release in smooth muscle cells of the guinea pig *taenia caeci*. *J. Gen. Physiol.*, **95**, 1103–1122.

Iino,M., Yamazawa,T., Miyashita,Y., Endo,M. and Kasai,H. (1993) Critical intracellular Ca^{2+} concentration for all-or-none Ca^{2+} spiking in single smooth muscle cells. *EMBO J.*, **12**, 5287–5291.

Jouaville,L.S., Ichas,F., Holmuhamedov,E.L., Camacho,P. and Lechleiter,J.D. (1995) Synchronization of calcium waves by mitochondrial substrates in *Xenopus laevis* oocytes. *Nature*, **377**, 438–441.

Kasai,H., Li,X.Y. and Miyashita,H. (1993) Subcellular distribution of Ca^{2+} release channels underlying Ca^{2+} waves and oscillations in exocrine pancreas. *Cell*, **74**, 669–677.

Lechleiter,J., Girard,S., Peralta,E. and Clapham,D. (1991) Spiral calcium wave propagation and annihilation in *Xenopus laevis* oocytes. *Science*, **252**, 123–126.

Lee,M.G., Xu,X., Zeng,W., Diaz,J., Wojcikiewicz,R.J., Kuo,T.H., Wuytack,F., Racymaekers,L. and Muallem,S. (1997) Polarized expression of Ca^{2+} channels in pancreatic and salivary gland cells. Correlation with initiation and propagation of $[Ca^{2+}]_i$ waves. *J. Biol. Chem.*, **272**, 15765–15770.

Li,W.H., Llopis,J., Whitney,M., Zlokarnik,G. and Tsien,R.Y. (1998) Cell-permeant caged IP_3 ester shows that Ca^{2+} spike frequency can optimize gene expression. *Nature*, **392**, 936–941.

Marchant,J.S., Callamaras,N. and Parker,I. (1999) Initiation of IP_3-mediated Ca^{2+} waves in *Xenopus* oocytes. *EMBO J.*, **18**, 5285–5299.

Newton,C.L., Mignery,G.A. and Südhof,T.C. (1994) Co-expression in vertebrate tissues and cell lines of multiple inositol-1,4,5-trisphosphate ($InsP_3$) receptors with distinct affinities for $InsP_3$. *J. Biol. Chem.*, **269**, 28613–28619.

Parker,I. and Ivorra,I. (1990) Inhibition by Ca^{2+} of inositol trisphosphate-mediated Ca^{2+} liberation: a possible mechanism for oscillatory release of Ca^{2+}. *Proc. Natl Acad. Sci. USA*, **87**, 260–264.

Parker,I. and Ivorra,I. (1993) Confocal microfluorimetry of Ca^{2+} signals evoked in *Xenopus* oocytes by photo-released inositol trisphosphate. *J. Physiol.*, **461**, 133–165.

Parker,I. and Yao,Y. (1991) Regenerative release of calcium from functionally discrete subcellular stores by inositol trisphosphate. *Proc. R. Soc. Lond. B Biol. Sci.*, **246**, 269–274.

Parker,I., Choi,J. and Yao,Y. (1996) Elementary events of $InsP_3$-induced Ca^{2+} liberation in *Xenopus* oocytes: hot spots, puffs and blips. *Cell Calcium*, **20**, 105–121.

Parys,J.B. and Bezprovanny,I. (1995) The inositol trisphosphate receptor of *Xenopus* oocyte. *Cell Calcium*, **18**, 353–363.

Pozzan,T., Rizzuto,R., Volpe,P. and Meldolesi,J. (1994) Molecular and cellular physiology of intracellular calcium stores. *Physiol. Rev.*, **74**, 595–636.

Rizzuto,R., Pinton,P., Brini,M., Chiesa,A., Filippin,L. and Pozzan,T. (1999) Mitochondria as biosensors of calcium microdomains. *Cell Calcium*, **26**, 193–199.

Rooney,T.A., Sass,E.J. and Thomas,A.P. (1990) Agonist-induced cytosolic calcium oscillations originate from a specific locus in single hepatocytes. *J. Biol. Chem.*, **265**, 10792–10796.

Simpson,P.B., Mehorta,S., Lange,G.D. and Russell,J.T. (1997) High density distribution of endoplasmic reticulum proteins and mitochondria at specialized Ca^{2+} release sites in oligodendrocyte processes. *J. Biol. Chem.*, **272**, 22654–22661.

Sun,X.-P., Callamaras,N., Marchant,J.S. and Parker,I. (1998) A continuum of $InsP_3$-mediated elementary Ca^{2+} signalling events in *Xenopus* oocytes. *J. Physiol.*, **509**, 67–80.

Swillens,S., Dupont,G., Combettes,L. and Champeil,P. (1999) From calcium blips to calcium puffs: theoretical analysis of the requirements for interchannel communication. *Proc. Natl Acad. Sci. USA*, **96**, 13750–13755.

Thomas,A.P., Bird,G.St.J., Hajnóczky,G, Robb-Gaspers,L.D. and Putney,J.W. (1996) Spatial and temporal aspects of cellular calcium signalling. *FASEB J.*, **10**, 1505–1517.

Thomas,D., Lipp,P., Berridge,M.J. and Bootman,M.D. (1998) Hormone-stimulated calcium puffs in non-excitable cells are not stereotypic, but reflect activation of different size channel clusters and variable recruitment of channels within a cluster. *J. Biol. Chem.*, **273**, 27130–27136.

Thomas,D., Lipp,P., Tovey,S.C., Berridge,M.J., Li,W., Tsien,R.Y. and Bootman,M.D. (2000) Microscopic properties of elementary Ca^{2+} release sites in non-excitable cells. *Curr. Biol.*, **10**, 1–8.

Thorn,P., Lawrie,A.M., Smith,P.M., Gallacher,D.V. and Petersen,O.H. (1993) Local and global cytosolic Ca^{2+} oscillations in exocrine cells evoked by agonists and inositol trisphosphate. *Cell*, **74**, 661–668.

Yao,Y. and Parker,I. (1994) Ca^{2+} influx modulates temporal and spatial patterns of inositol-trisphosphate-mediated Ca^{2+} liberation in *Xenopus* oocytes. *J. Physiol.*, **476**, 17–28.

Yao,Y., Choi,J. and Parker,I. (1995) Quantal puffs of intracellular Ca^{2+} evoked by inositol trisphosphate in *Xenopus* oocytes. *J. Physiol.*, **482**, 533–553.

Received September 27, 2000; revised and accepted November 13, 2000